Etching of Plasma-Polymerized Tetrafluoroethylene, Polytetrafluoroethylene, and Sputtered Polytetrafluoroethylene Induced by Atomic Oxygen [O(^{3}P)]*

THEODORE WYDEVEN, MORTON A. GOLUB, and NARCINDA R. LERNER, *Ames Research Center, NASA, Moffett Field, California 94035*

Synopsis

A study was carried out of the surface recession (etching) of thin films of plasma-polymerized tetrafluoroethylene (PPTFE), polytetrafluoroethylene (PTFE), and ion-beam sputter-deposited polytetrafluoroethylene (SPTFE), exposed to atomic oxygen [O(^{3}P)] downstream from a nonequilibrium radio-frequency O_2 plasma. At 22°C, the etch rates for PTFE, SPTFE, and PPTFE were in the ratio of 8.7 : 1.8 : 1.0. A thin, conformal coating of PPTFE (etch rate of 0.3 nm/h at 22°C) was found to protect an underlying, cast film of a reactive polymer, *cis*-1,4-polybutadiene (etch rate of 0.13 mg/cm^2 h ≡ 1300 nm/h at 22°C), against O(^{3}P) attack for the time required to fully etch away the PPTFE coating. From ESCA analysis, PTFE exhibited only minor surface oxidation (uptake of 0.5 atom % O) upon etching, its F/C ratio decreasing slightly from 2.00 to 1.97; PPTFE exhibited considerable surface oxidation (uptake of 5.9 atom % O) and a decrease in F/C ratio from 1.30 to 1.23; and SPTFE exhibited a surface oxidation (uptake of 2.2 atom % O) intermediate between those of PTFE and PPTFE, with a decrease in F/C ratio from 1.73 to 1.67. The O(^{3}P)-induced etching of PTFE had an activation energy of 3.8 kcal/mol, but no activation energy value was obtained for PPTFE which gave a nonlinear Arrhenius plot apparently because of thermally induced thinning above 50°C.

INTRODUCTION

Considerable interest has been shown in the surface recession (etching) of polymers exposed to ground-state atomic oxygen [O(^{3}P)] in low Earth orbital environment,[1-5] and some effort has been devoted to seeking protective coatings for space applications.[6] Previously, we reported that polybutadienes and related unsaturated hydrocarbon polymers are quite reactive towards O(^{3}P) generated by a radio-frequency glow discharge in O_2, the etch rates for these polymers being dependent upon polymer structure.[7] Since Teflon (PTFE) was reported to be very resistant to O(^{3}P)-induced etching in the space environment,[1] it seemed reasonable to expect that plasma-polymerized tetrafluoroethylene (PPTFE), a highly branched and crosslinked polymer[8] (with a fluorine/carbon ratio of 1.3–1.4, in contrast to 2.0 for the linear PTFE polymer), would also be resistant. Indeed, since crosslinked natural rubber had been reported to be much more resistant to O_2 plasma etching than the corresponding uncrosslinked polyisoprene,[9] the possibility exists that PPTFE

*Presented at 8th International Symposium on Plasma Chemistry, Tokyo, Japan, Aug. 31–Sept. 4, 1987.

Journal of Applied Polymer Science, Vol. 37, 3343–3355 (1989)
Not subject to copyright within the United States.
Published by John Wiley & Sons, Inc. CCC 0021-8995/89/123343-13$04.00

might even be more resistant than PTFE. Thus, PPTFE films, if found to be particularly resistant to $O(^3P)$ attack, could be used as protective coatings for vulnerable polymers that may be deployed in space. Such films are easily deposited on various substrates,[10] and plasma-polymerized coatings have received much attention.[11] In this paper, we report on the $O(^3P)$-induced etching of PPTFE, PTFE, and an ion-beam sputter-deposited[6] PTFE (SPTFE, with $F/C = 1.7$), using ESCA to follow surface structural changes produced in these polymers. We also demonstrate that thin films of PPTFE can protect *cis*-1,4-polybutadiene (CB) against $O(^3P)$-induced etching.

EXPERIMENTAL

PTFE film (25-μm thick) was donated by Chemical Fabrics Corp., West Palm Beach, FL. A 533-nm film of SPTFE (on a silicon substrate) was kindly supplied by Bruce A. Banks, Lewis Research Center, Cleveland, OH. Tetrafluoroethylene monomer (TFE) inhibited with *d*-limonene (SCM Specialty Chemicals, Gainesville, FL) was used without further purification to prepare PPTFE. PPTFE films were deposited on the polished surfaces of small square sections (1.42 cm^2) of silicon cut from an Si wafer, using the plasma polymerization reactor described previously.[12] The following conditions were used for PPTFE deposition:

Power: 10 W at 13.56 MHz
TFE flow rate: 0.5 cm^3 (STP)/min
Pressure: 76 Pa (0.57 torr), discharge off
Deposition rate: 0.066 nm/s

The thickness and refractive index of the PPTFE films (on Si), before and after etching, were measured with a Gaertner Model L116 automatic ellipsometer. The refactive index at 632.8 nm before etching was 1.374 ± 0.002, and the density, determined from thickness and weight-gain measurements on Si substrates of known area, was 2.3 ± 0.1 g/cm^3. The etching of PPTFE, measured in nm, was expressed as mg/cm^2, after multiplying the thinning (in cm) by the density (in mg/cm^3). The etching of SPTFE at 22°C was similarly followed by ellipsometry. Weight loss in the PTFE films (disks cut to area of 2.54 cm^2) was measured on a Cahn Model 26 automatic electrobalance and likewise expressed as mg/cm^2.

The $O(^3P)$ reactor was described previously.[7] The O_2 and O atom flow rates (the latter obtained by titration with NO_2) were 3.9 and 1.4 cm^3 (STP)/min, respectively, and the O atom partial pressure was 0.17 torr at the NO_2 titration port. For etching at elevated temperatures, the reactor was heated either by a heating tape or by water passing thrugh copper coils located inside a Dewar surrounding the sample holder. Temperature was measured with a thermocouple having a junction located beneath the sample support. ESCA analysis was performed on a Surface Science Instruments SSX-101 spectrometer, using Teflon tape as a standard, and the binding energies of PPTFE and SPTFE given here were referenced for the single F_{1s} peak of $-\overset{|}{C}F-/-CF_2-/-CF_3$ at 689.2 eV.

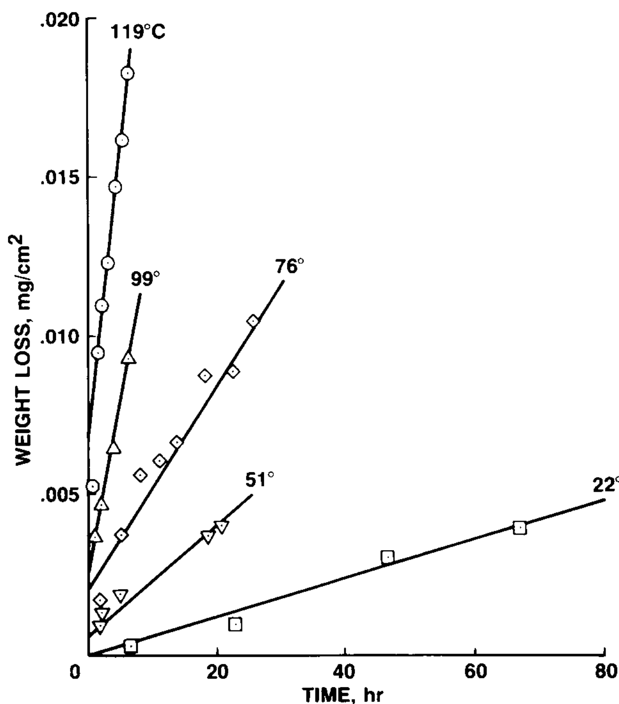

Fig. 1. Typical kinetic plots for $O(^3P)$-induced etching of PPTFE films at different temperatures.

To demonstrate the protectiveness imparted by PPTFE coatings, an Si substrate and a CB film (cast onto a glass cover slip[7]) were simultaneously exposed to TFE for the same length of time in the plasma polymerization reactor. The resulting PPTFE coatings—assumed to have the same thickness on Si and on CB—were each subjected to $O(^3P)$ for various periods of time; thickness measurements were made on the former coating until the PPTFE was completely etched away, while weight-loss measurements were made on the latter coating to record the onset and subsequent etching of CB.

RESULTS AND DISCUSSION

Typical kinetic plots for $O(^3P)$-induced surface recession, or etching, of PPTFE and PTFE films at various temperatures are shown in Figures 1 and 2. The etching plots for PPTFE at elevated temperatures—after initial, rapid decreases in thickness—are essentially linear but have different intercepts; the etching plots for PTFE are linear and pass thrugh the origin at all temperatures. The slopes of the straight-line plots of Figures 1 and 2 were used to construct the Arrhenius plots presented in Figure 3; the activation energy for $O(^3P)$-induced etching of PTFE was found to be 3.8 kcal/mol by a least squares fit to an Arrhenius expression, but no activation energy could be determined for PPTFE because of its nonlinear Arrhenius plot. This nonlinearity apparently arises because PPTFE undergoes a thermally induced thinning in the absence of $O(^3P)$, which becomes increasingly significant as the temperature is raised above 50°C and which contributes to the overall thin-

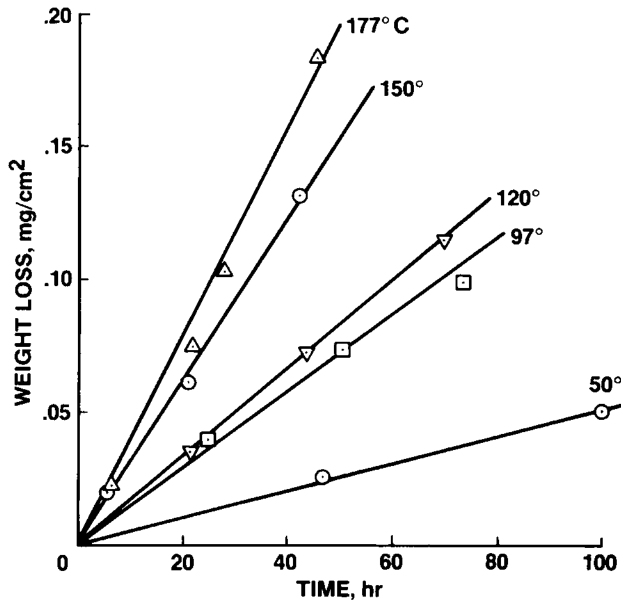

Fig. 2. Typical kinetic plots for $O(^3P)$-induced etching of PTFE films at different temperatures.

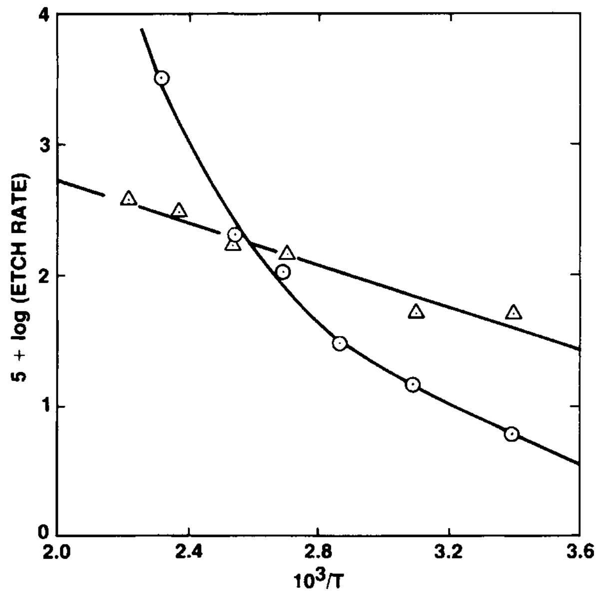

Fig. 3. Arrhenius plots for $O(^3P)$-induced etching of PTFE (△) and PPTFE (○) films. Etch rates were calculated in units of mg/cm^2 h.

ning in the presence of $O(^3P)$ at elevated temperatures. The PPTFE intercepts may represent different extents of loss of low molecular weight byproducts of the plasma polymerization of TFE contained within the PPTFE matrix. PTFE, on the other hand, is thermally stable in the temperature region of interest and hence yielded a normal Arrhenius plot.

At 22°C, the etch rate for PTFE (5.3×10^{-4} mg/cm^2 h) is seen to be 8.7 times that of PPTFE (6.1×10^{-5} mg/cm^2 h) (Fig. 3). In view of what was stated in the Introduction, the higher resistance of PPTFE to $O(^3P)$-induced etching at ambient temperature is ascribed to its crosslinked structure,[8] whereas PTFE has a linear structure. Interestingly, SPTFE was found to have an etch rate at 22°C (1.1×10^{-4} mg/cm^2 h; kinetic plot not shown here) that is 1.8 times that of PPTFE but only 0.21 times that of PPTFE. That SPTFE has an etch rate much closer to that of PPTFE than to that of PTFE is not surprising since ion-beam sputtering of PTFE involves breakdown of the latter's linear polymer structure and reconstitution elsewhere of a polymer network from the PTFE fragments. However, while various workers[13,14] noted that argon plasma sputtering of PTFE yields a structure comparable to that of the highly crosslinked PPTFE, our ion-beam sputter-deposited PTFE has a structure (based on ESCA results given below) that is less crosslinked than PPTFE and contains short sequences of CF_2 groups. At any rate, the significantly lower etch rate for SPTFE compared to PTFE reinforces the viewpoint that crosslinking enhances resistance to $O(^3P)$-induced etching of an otherwise linear polymer.

The protectiveness of a very thin PPTFE coating against $O(^3P)$-induced etching at ambient temperature is illustrated in Figure 4 by means of two PPTFE coatings having the same initial thickness (16.8 nm)—one deposited onto an Si substrate (for following decrease in thickness), the other onto a CB film cast on a glass cover slip (for following weight loss). As may be seen, the onset of significant weight loss in the PPTFE/CB sample occurs only after a time interval (~ 50–60 h) required for the PPTFE coating to be nearly completely etched away (the weight of the PPTFE coating being immeasurable in this sample). This is demonstrated by the fact that the PPTFE/Si sample reaches a negligible thickness (0.2 nm) after this same time interval. In fact, the "breakthrough" point is in good agreement with the predicted value of about 62 h, given an etch rate for PPTFE of 0.27 nm/h ($\equiv 6.1 \times 10^{-5}$ mg/cm^2 h) at 22°C (Figs. 1 and 3). Moreover, the sharp rise in the weight-loss curve of PPTFE/CB, subsequent to the removal of the PPTFE coating, yields an etch rate for CB of 0.18 mg/cm^2 h, which agrees quite well with the previously reported etch rate of 0.13 mg/cm^2 h for CB in the same $O(^3P)$ reactor.[7] The near constant weight of the PPTFE/CB sample prior to total removal of the PPTFE coating indicates that oxygen atoms do not diffuse into PPTFE to any significant extent. At the same time, it implies that the PPTFE coating is conformal and free of pinholes.

The C_{1s} and O_{1s} regions of the ESCA spectra of PPTFE films before and after etching at 22°C are shown in Figures 5 and 6. The analytical data are summarized in Table I, where the estimated accuracy of each deconvoluted peak area (given in parentheses) is $\pm 5\%$ of its given value, while the estimated accuracy of each F/C ratio is $\pm 2\%$ of its given value. Since the F_{1s} regions were unchanged and, moreover, resembled the single intense peak at 689.2 eV

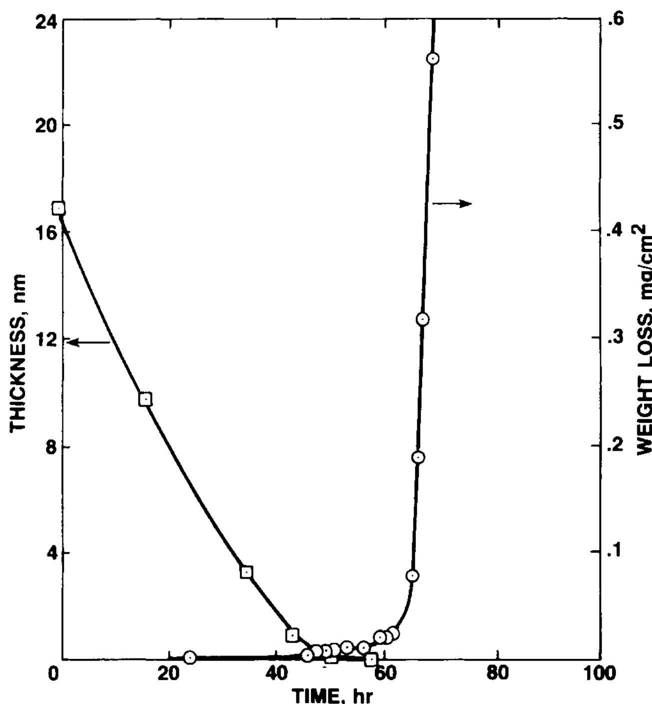

Fig. 4. Protective effect imparted by a PPTFE coating against O(^{3}P) attack at 22°C (see text): (□) thinning of a PPTFE coating on Si substrate; (○) weight loss in a PPTFE coating on a CB film cast on a glass cover slip. Both PPTFE coatings had the same initial thickness (16.8 nm).

($-CF_x$) in the ESCA spectra of PPTFE[14] or of Teflon, there was no need to show them here. The C_{1s} spectrum of unetched PPTFE is very similar to the spectra of polymers obtained by various workers[14-17] from in-glow plasma polymerization of TFE in showing the same four prominent peaks with roughly the same relative intensities. However, these C_{1s} spectra differ from that of a PPTFE produced in nonglow regions,[18] which approaches that of ordinary PTFE with its single $-CF_2-$ peak. There is universal agreement on the PPTFE assignments[14-17,19] shown in Figure 5(A), and the weak peak around 285 eV signifies a small amount of hydrocarbon contamination.[16] To the extent that oxidation of the PPTFE surface occurs on exposure to O(^{3}P), we should consider that the various C_{1s} peaks in Figure 5(B) contain, besides the functional groups indicated in Figure 5(A), unknown amounts of C atoms attached to O atoms: $-CF_2-O-$ (294.1) and $-\overset{|}{C}F-O-$ (292.0 eV), as well as C atoms in $\diagdown C{=}O$ (288.1–288.9) and $\gtrdot C-O-$ (286.7–287.5 eV), where the latter two groups are attached to one or two $-CF_x$ groups (see footnotes in Table I). These four assignments are based on unpublished ESCA data on perfluoroethers and appropriate model compounds.[20] In addition, the ESCA spectra in Figure 5 are assumed to contain an undetermined amount of carbon atoms attached to double bonds (as in $=C\langle$, $=CF-$, or $=CF_2$ unsaturation),[16] which could comprise some 20% of the total carbon content in the unetched PPTFE[21]; however, their exact locations under the various peaks cannot be specified. Consequently, the data in Table I should be

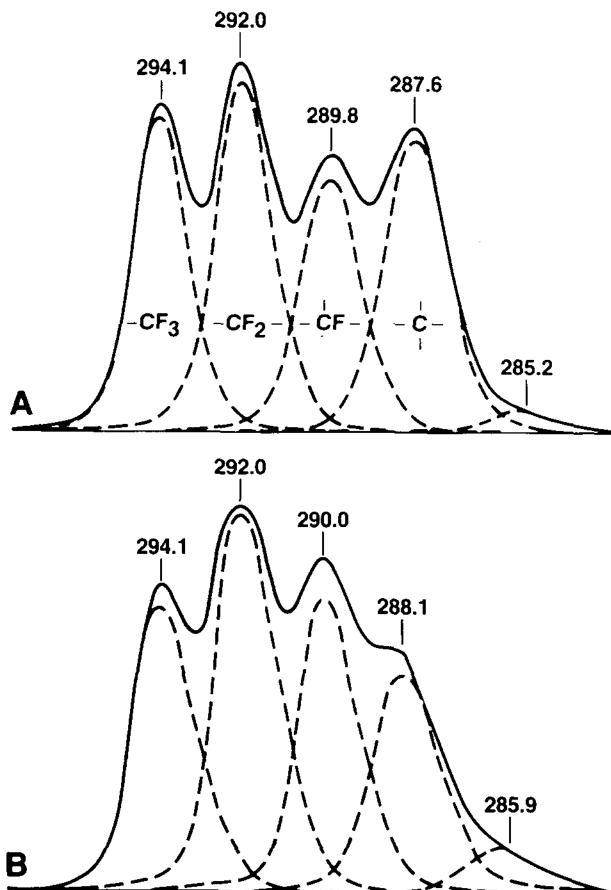

Fig. 5. C_{1s} regions of ESCA spectra of PPTFE before (A) and after (B) $O(^3P)$-induced etching. Assignments of peaks under B are the same as those under A, except for additional groups indicated in footnotes of Table I. Binding energies in this and the following figures are given in eV units.

considered to have only semiquantitative significance, but they do point to a small decrease in the F/C ratio for PPTFE from 1.30 to 1.23 as a result of etching. It should be noted that these F/C ratios were determined by dividing the area under the F_{1s} peak by the total area under the five C_{1s} peaks (shown in Fig. 5), and adjusting the number by a sensitivity factor which accounts for the different cross sections for photoionization of F and C atoms; another method, which involves calculating the F/C ratio from the percentage of each group present in the C_{1s} region and which is believed to be less reliable, typically yields ratios higher by 0.2–0.4 than those calculated by the former method.[22] This accounts for the fact that the C_{1s} data in Table I for unetched PPTFE yield an F/C ratio by the second method, viz., 1.45, which is higher than that given in the table. The existence of C=C groups in PPTFE, which could give rise to overlapping "satellite" contributions to the CF_3 peak,[22] may be largely responsible for the discrepancy in F/C ratios obtained by the two methods.

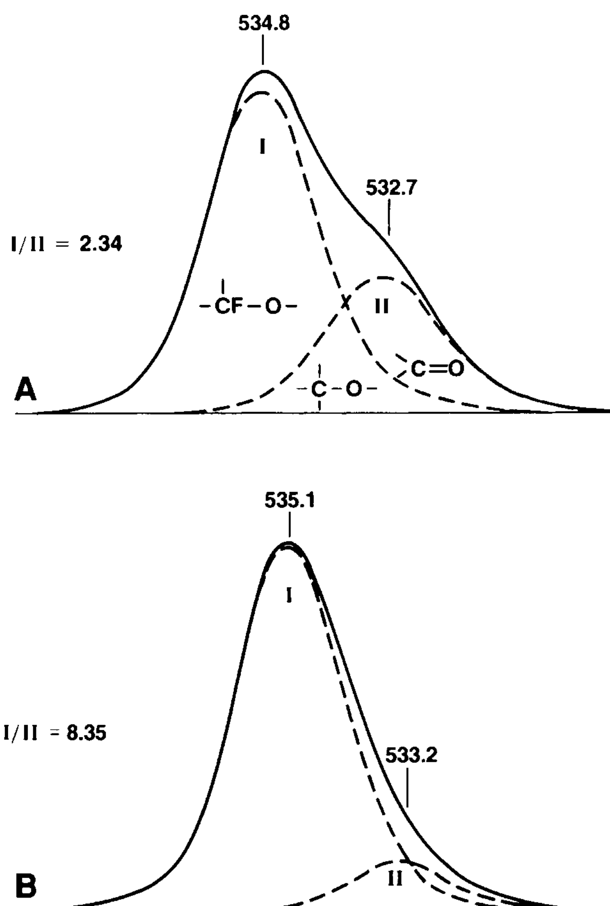

Fig. 6. O_{1s} regions of ESCA spectra of PPTFE before (A) and after (B) $O(^3P)$-induced etching. Spectra are not to scale; area under B corresponds to 8.4 times area under A.

Inspection of the ESCA spectra in Figures 5 and 6 and of the data in Table I suggests the following trends in surface structural changes in PPTFE as a result of etching: (1) a decrease of 3.2 atom % in the concentration of $-\overset{|}{\underset{|}{C}}-/ >C{=}O, \geqslant C-O-$ (peaks at 287.6 and 288.1 eV), accompanied by only a 0.5 atom % increase in $\geqslant C{=}O / \geqslant C-O-$ (peaks at 532.7 and 533.2 eV); (2) slight increases in $-\overset{|}{C}F-/ \geqslant C{=}O$ (peaks at 289.8 and 290.0 eV) and in $-CF_2-/-\overset{|}{C}F-O-$ (peaks at 292.0 eV in both etched and unetched spectra); (3) slight decrease in $-CF_3/-CF_2-O-$ (peaks at 294.1 eV); (4) a large increase of 5.4 atom % in O bound to fluorinated C (peaks 534.8 and 535.1 eV); (5) a total uptake of 5.9 atom % O (i.e., from 0.8 to 6.7 atom % O in Table I), accompanied by a decrease of 4.6 atom % F and by a slight decrease in C (from 43.2 to 41.9 atom % C). These surface structural changes, of course, occur even as the surface is being eroded, constantly

TABLE I
Atom (and Peak Area) % Distribution in ESCA Spectra of PPTFE[a]

Condition	C_{1s} peaks					O_{1s} peaks		F_{1s} peak	
	$-CF_3$	$-CF_2-$	$-\overset{\vert}{C}F-$	$-\overset{\vert}{\underset{\vert}{C}}-$	$-CH_2-$	$-\overset{\vert}{C}F-O-$	$>C=O$	$-CF_2-$	F/C
Unetched	9.9	11.9	9.3	11.3	0.8	0.6	0.2[b]	56.0	1.30
	(23.0	27.6	21.5	26.2	1.7)	(70.1	29.9)	(100.0)	
Etched	9.5[c]	13.1[d]	9.8[e]	8.1[e,f]	1.4[f]	6.0	0.7[b]	51.4	1.23
	(22.6	31.2	23.5	19.3	3.4)	(89.3	10.7)	(100.0)	

[a] Extent of etching at 22°C: ~ 9.5 nm.
[b] May include some $>C-O-$.
[c] May include some $-CF_2-O-$.
[d] May include some $-\overset{\vert}{C}F-O-$.
[e] May include some $>C=O$.
[f] May include some $>C-O-$.

regenerating fresh surface. Unfortunately, it is not possible at this time to offer a detailed picture of the O(^{3}P)-induced oxidative etching of PPTFE. However, any addition of O atoms to perfluoroolefinic double bonds, to the extent that it results in stable adducts in PPTFE as opposed to degradation processes yielding CF_2O and assorted products,[23] will not alter the F/C ratio and, hence, will not affect the above argument concerning changes in the atom % distributions.

PTFE, in contrast to PPTFE, showed relatively little oxygen uptake on exposure to O(^{3}P), despite a more rapid rate of etching at 22°C: the ESCA spectrum for a film of PTFE etched to the extent of 0.4 μm showed only 0.47 atom % O (with an F/C ratio of 1.97), while the spectrum of the unetched PTFE (F/C = 2.00) showed no oxygen at all. Since the C_{1s} and F_{1s} spectra of PTFE before and after etching appeared unchanged (each exhibiting single peaks at 292.2 and 689.2 eV, respectively), they were omitted here. Likewise, the O_{1s} spectrum of etched PTFE, which showed only a single peak at 532.3 eV ($>C=O$), was also omitted.

Since the infrared spectrum of PPTFE obtained in this study closely resembled those of PPTFE reported in the literature[10,24-26] there was no need to show it here. It is sufficient to note the presence of a strong, broad band at 900–1500 cm^{-1} and centered at 1220 cm^{-1} ($-CF_2-$), a weak band at 740 cm^{-1} ("amorphous" $-CF_2-$ structure[26]), a weak, broad band at 1720 cm^{-1} ($>C=O$, $-CF=CF-$ groups[17]), and a very weak shoulder at 1780 cm^{-1} ($-CF=CF_2$ unsaturation[17]). The presence of unsaturation in PPTFE had also been recognized by means of solid-state ^{13}C NMR analysis,[16] but it could not be assessed by ESCA analysis.[16] For plausible models of the PPTFE structure, the reader may inspect Refs. 24 and 27.

The C_{1s} and O_{1s} ESCA spectra of SPTFE before and after etching at 22°C are shown in Figures 7 and 8, and the analytical data are summarized in Table II. Here again, there was no need to show the corresponding F_{1s} spectra for SPTFE, since they each possessed but a single peak at 689.2 eV, in common

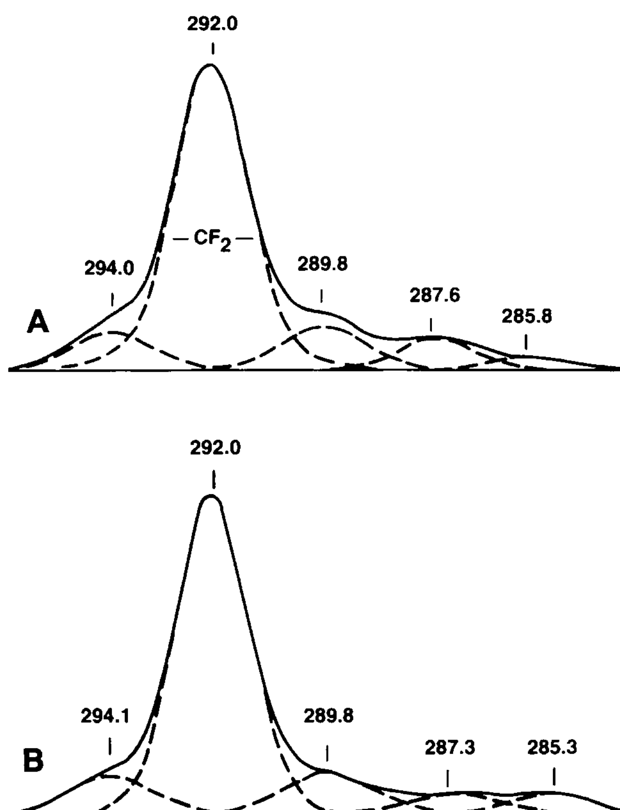

Fig. 7. C_{1s} regions of ESCA spectra of SPTFE before (A) and after (B) $O(^3P)$-induced etching. Assignments of peaks under A and B are the same as those indicated for Figures 5(A) and 5(B).

with the F_{1s} spectra of PTFE and PPTFE. It is obvious from Figure 7 that the C_{1s} spectra of the unetched and etched SPTFE each have the appearance of a composite of the corresponding spectra of PTFE (with a single $-CF_2-$ peak at 292.0 eV) and of PPTFE (with its four prominent peaks), the latter two polymers *seeming* to be present in the approximate ratio of 4–5 : 1. This observation implies that our SPTFE must be considerably less crosslinked than the highly crosslinked PPTFE. Our SPTFE also contrasts sharply with an argon plasma-sputtered PTFE (reported recently by Sugimoto and Miyake[28]), the C_{1s} spectrum of which is very similar to that of our PPTFE and which therefore signifies a very high degree of crosslinking in the cited SPTFE. That our SPTFE has only a slightly modified PTFE structure was supported by an ATR–IR spectrum (not shown here) which exhibited no absorption bands of consequence other than the strong doublet at 1157 and 1215 cm^{-1}, characteristic of the $C-F$ asymmetric and symmetric stretching vibrations, respectively, of linear PTFE.[29]

Since the changes observed in the C_{1s} spectra of PPTFE as a result of $O(^3P)$-induced etching (Fig. 5) are not dramatic, and since no changes were observed in the C_{1s} spectra of PTFE (as mentioned earlier), it is not surprising that the C_{1s} spectral changes in SPTFE (Fig. 7) upon etching are rather slight.

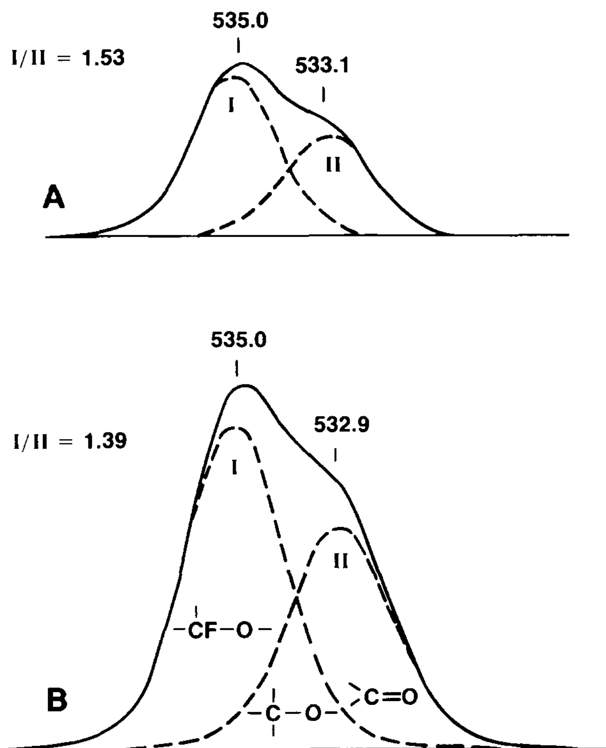

Fig. 8. O_{1s} regions of ESCA spectra of SPTFE before (A) and after (B) $O(^3P)$-induced etching. Spectra are not to scale; area under B corresponds to 5.4 times area under A.

TABLE II
Atom (and Peak Area) % Distribution in ESCA Spectra of SPTFE[a]

Condition	C_{1s} peaks					O_{1s} peaks		F_{1s} peak	F/C
	$-CF_3$	$-CF_2-$	$-\overset{\vert}{C}F-$	$-\overset{\vert}{\underset{\vert}{C}}-$	$-CH_2-$	$-\overset{\vert}{C}F-O-$	$>C=O$	$-CF_2-$	
Unetched	3.2	25.4	4.1	2.8	1.0	0.3	0.2	63.0	1.73
	(8.7	69.8	11.4	7.5	2.6)	(60.4	39.6)	(100.0)	
Etched	3.1[b]	26.4[c]	3.6[d]	1.8[d, e]	1.6[e]	1.6	1.1[f]	60.8	1.67
	(8.6	72.1	9.8	5.0	4.5)	(58.1	41.9)	(100.0)	

[a] Extent of etching at 22°C: ~ 48 nm.
[b] May include some $-CF_2-O-$.
[c] May include some $-\overset{\vert}{C}F-O-$.
[d] May include some $>C=O$.
[e] May include some $>C-O-$.
[f] May include some $>C-O-$.

However, the changes in the atom % distribution of the C_{1s} peaks for SPTFE (Table II) largely parallel corresponding changes in PPTFE (Table I). On the other hand, the changes in the O_{1s} spectra of SPTFE do not follow the pattern for PPTFE: Whereas the ratio of areas of the two peaks I and II in Figure 6 increases considerably from 2.34 to 8.35, the corresponding ratio in Figure 8 decreases slightly from 1.53 to 1.39. This difference is no doubt related to SPTFE having a structure that is some 75–80% like that of PTFE and some 20–25% like that of PPTFE. Thus, for an oxygen uptake in SPTFE of 2.2 atom % (i.e., 2.7–0.5 atom % O in Table II), about 0.9/2.2, or 40%, of the oxidation presumably occurs at PTFE segments to produce the peak at 532.9 eV [Fig. 8(B)], given the prior observation that etched PTFE showed a single O_{1s} peak around 532.3 eV; the remaining 60% of the oxidation can be considered to occur at PPTFE branch points and/or crosslinks to produce the peak at 535.0 eV, given the dominance of the 535.1-eV peak in the O_{1s} spectrum of etched PPTFE [Fig. 6(B)]. Again reflecting the mixed PTFE/PPTFE structure of SPTFE, it is worth recalling that the oxygen uptakes in PPTFE, SPTFE, and PTFE—after sufficient etching time to reach "equilibrium" oxidized surfaces—were 5.9, 2.2, and ~ 0.5 atom % O, respectively. In future work, it would be interesting to examine a series of SPTFE specimens prepared under different degrees of severity of sputtering to see how the etch rates and oxygen uptakes varied with network structure. Meanwhile, we should note again that our SPTFE, with an initial F/C ratio of 1.73, had an etch rate that was about 2/9 of that of PTFE (with an F/C ratio of 2.0) and about twice that of PPTFE (with an initial F/C ratio of 1.30).

The authors are indebted to R. D. Cormia of Surface Science Laboratories, Inc., Mountain View, CA, for having provided ESCA spectra of PTFE, PPTFE, and SPTFE, and their interpretation.

References

1. L. J. Leger and J. T. Visentine, *J. Spacecraft Rockets*, **23**, 505 (1986); L. Leger, J. Visentine, and B. Santos-Mason, *Int. SAMPE Tech. Conf.*, **18**, 1015 (1986); and references cited therein.
2. G. S. Arnold and D. R. Peplinski, *AIAA J.*, **23**, 1621 (1985); and references cited therein.
3. D. G. Zimcik, R. C. Tennyson, L. J. Kok, and C. R. Maag, *Eur. Space Agency Spec. Publ.*, *1985*, ESA SP-232, pp. 81–89; *Chem. Abstr.*, **104**, 149894 (1986); and references cited therein.
4. L. P. Torre and H. G. Pippin, *Int. SAMPE Tech. Conf.*, **18**, 1086 (1986).
5. M. McCargo, R. A. Dammann, T. Cummings, and C. Carpenter, *Eur. Space Agency Spec. Publ.*, *1985*, ESA SP-232, pp. 91–97; *Chem. Abstr.*, **104**, 226351 (1986).
6. B. A. Banks, M. J. Mirtich, S. K. Rutledge, and D. M. Swec, *Thin Solid Films*, **127**, 107 (1985).
7. M. A. Golub, N. R. Lerner, and T. Wydeven, *Am. Chem. Soc. Symp. Ser.*, **364**, 342 (1987).
8. H. Yasuda and T. Hsu, *Surf. Sci.*, **76**, 232 (1978).
9. R. H. Hansen, J. V. Pascale, T. De Benedictis, and P. M. Rentzepis, *J. Polym. Sci.*, **A3**, 2205 (1965).
10. T. Wydeven and C. C. Johnson, *Polym. Eng. Sci.*, **21**, 650 (1981).
11. H. Yasuda, *Plasma Polymerization*, Academic, Orlando, 1985.
12. T. Wydeven, *Appl. Opt.*, **16**, 717 (1977).
13. J. M. Tibbitt, M. Shen, and A. T. Bell, *Thin Solid Films*, **29**, L43 (1975).
14. A. Dilks and E. Kay, *Macromolecules*, **14**, 855 (1981).
15. D. W. Rice and D. F. O'Kane, *J. Electrochem. Soc.*, **123**, 1308 (1976).

16. S. Kaplan and A. Dilks, *J. Appl. Polym. Sci., Appl. Polym. Symp.*, **38**, 105 (1984).
17. N. Inagaki, T. Nakanishi, and K. Katsuura, *Polym. Bull (Berlin)*, **9**, 502 (1983).
18. D. F. O'Kane and D. W. Rice, *J. Macromol. Sci., Chem.*, **A10**, 567 (1976).
19. K. Nakajima, A. T. Bell, M. Shen, and M. M. Millard, *J. Appl. Polym. Sci.*, **23**, 2627 (1979).
20. R. D. Cormia, private communication.
21. J. Perrin and R. Dandoloff, *J. Non-Cryst. Solids*, **86**, 179 (1986).
22. P. D. Buzzard, D. S. Soong, and A. T. Bell, *J. Appl. Polym. Sci.*, **27**, 3965 (1982).
23. R. E. Huie and J. T. Herron, *Prog. Reaction Kinetics*, **8**, 1 (1980).
24. K. Hozumi, K. Kitamura, and T. Kitade, *Bull. Chem. Soc. Jpn.*, **54**, 1392 (1981).
25. J. M. Tibbitt, A. T. Bell, and M. Shen, *J. Macromol. Sci., Chem.*, **A10**, 519 (1976).
26. U. Hetzler and E. Kay, *J. Appl. Phys.*, **49**, 5617 (1978).
27. J. Chen, Z. Chen, and Z. Wang, *Kobunshi Ronbonshu*, **41**, 705 (1984).
28. I. Sugimoto and S. Miyake, Paper No. AII-07, 8th Int. Symp. on Plasma Chem., Tokyo, 1987, pp. 1334–1339.
29. D. I. McCane, *Encycl. Polym. Sci. Technol.*, **13**, 623 (1970).

Received March 7, 1988
Accepted June 1, 1988